Karl Hess

"Advanced Theory of Semiconductor Devices"

(IEEE Press, 1999)

CHAPTER 5

EQUILIBRIUM STATISTICS FOR ELECTRONS AND HOLES

Although we discussed the energy band structure (the electronic states) of a semiconductor in detail in the previous chapters, we did not include in our discussion whether these states are actually filled with electrons (two with opposite spin in each state are possible) or not.

In Chapter 4 we have shown, however, that full bands do not contribute to the electronic current. In a defect-free semiconductor at $T = 0$, all bands up to the so-called conduction band are filled. The last filled band is the valence band. As the temperature increases, electrons from the valence band will be excited to the conduction band, and the electrons and holes generated in this way will be able to conduct a current (not as large as in a metal where valence and conduction bands overlap). We also can introduce electrons and holes by doping. To compute the conductivity, we need to know which states are occupied and which are empty. This knowledge is usually acquired by calculating the probability that a state is occupied and by calculating the density of states. The actual carrier occupation is then proportional to the product of these two quantities, which are treated separately below.

5.1 DENSITY OF STATES

Consider a crystal with periodic boundary conditions and N atoms along each of the main coordinate axes. Then, according to Eq. (2.19), the allowed wave vectors are given by

$$\mathbf{k} = \frac{\mathbf{K}_h}{N} = \frac{h_1}{N}\mathbf{b}_1 + \frac{h_2}{N}\mathbf{b}_2 + \frac{h_3}{N}\mathbf{b}_3 \tag{5.1}$$

with

$$0 \leq |h_i| \leq N/2$$

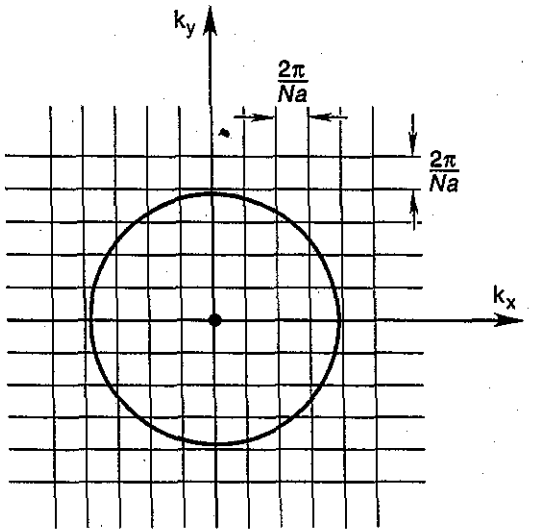

Figure 5.1 Allowed values for the **k** vector in two dimensions.

In a simple cubic crystal, $\mathbf{b}_1$ would be of the form $2\pi/a$ times unit vector (and similarly $\mathbf{b}_2$ and $\mathbf{b}_3$), and therefore, the typical form of **k** is

$$\mathbf{k} = \frac{2\pi h_1}{Na} \times \text{unit vector} + \ldots \tag{5.2}$$

The components of the allowed **k** values form the "lattice" shown in Figure 5.1, where $Na = L$ is the length of the crystal in each direction.

This treatment involving the crystal length and the periodic boundary conditions, may seem somewhat artificial. However, because the end results will not depend on the quantities (N, L, etc.) connected to these artificial conditions, we need not be concerned about it. It is the advantage of periodic boundary conditions that their proper application always gives correct results for bulk properties. Of course, they are invalid when surface properties become important.

We are interested in the number of states at the energy E in the interval $[E, E+dE]$. To calculate this number, we first assume the simple case of *spherical* constant energy surfaces in **k** space. The number of allowed **k** values in the sphere in Figure 5.1 is then equal to the number of cubes of side length $2\pi/L$ in the sphere. The volume $V_{\mathbf{k}}$ of the sphere is

$$V_{\mathbf{k}} = \frac{4\pi}{3}k^3 = \frac{4\pi}{3}\left[\frac{2m^*(E-E_c)}{\hbar^2}\right]^{3/2} \tag{5.3}$$

The number of states $\bar{N}(E)$ in this volume is

$$\bar{N}(E) = V_{\mathbf{k}} / \left(\frac{2\pi}{L}\right)^3 \tag{5.4}$$

For systems other than simple cubic, one replaces the cubes of reciprocal volume $(\frac{2\pi}{L})^3$ by other unit cells. The outcome is the same.

Because each state can be occupied with two electrons of opposite spin, the number $N(E)$, which finally tells us how many electrons can be accommodated, is twice as large as $\bar{N}(E)$

$$N(E) = 2\bar{N}(E) \tag{5.5}$$

As can be seen from the following algebra, the quantity that is most useful is the number of states per unit sample volume at energy E in the interval $[E, E+dE]$. This quantity is called the density of states $g(E)$, which is given by

$$g(E) = \frac{1}{L^3}\frac{dN(E)}{dE} = \frac{1}{2\pi^2}\left(\frac{2m^*}{\hbar^2}\right)^{3/2}\sqrt{E-E_c} \tag{5.6}$$

To understand the importance of $g(E)$, let us assume for the moment that we know the probability $f(E)$ that an electron occupies a state with energy E. Then we can obtain the density n_c of electrons in the conduction band from

$$n_c = \sum_{\mathbf{k}} f(E) = \int_{E_c}^{\infty} f(E)g(E)\,dE \tag{5.7}$$

Equation (5.6) can be derived also in a different way: Because the allowed **k** values are separated from each other only by very small distances (L is very large), the summation $\sum$ can be replaced by an integration $\int d\mathbf{k}$. Because the number of **k** values in the volume $d\mathbf{k} = dk_x\,dk_y\,dk_z$ is equal to $d\mathbf{k}/(2\pi/L)^3$, we obtain the number per unit volume (including a factor of 2 for the spin) as

$$2\left(\frac{1}{2\pi}\right)^3 d\mathbf{k}$$

and we have

$$\frac{1}{V_{\text{ol}}}\sum_{\mathbf{k}} \to 2\int\left(\frac{1}{2\pi}\right)^3 d\mathbf{k} \tag{5.8}$$

Using spherical coordinates, we obtain

$$dk_x\,dk_y\,dk_z = k^2 dk \sin\theta\, d\theta\, d\phi \tag{5.9}$$

It is then easy to show that

$$\frac{2}{(2\pi)^3}\int d\mathbf{k} \to \int g(E)\,dE \tag{5.10}$$

For complicated $E(\mathbf{k})$ relations, $g(E)$ takes a form that is more complicated than Eq. (5.6). For example, for one of the lowest conduction band [illegible]ma in silicon

(one of the six ellipsoids), we have (transforming the ellipsoid to a sphere by a suitable coordinate transformation in **k** space)

$$g(E) = \frac{\sqrt{m_l^* m_t^{*2}}}{2\pi^2}\left(\frac{2}{\hbar^2}\right)^{3/2}\sqrt{E - E_c} \tag{5.11}$$

The term $\sqrt{m_l^* m_t^{*2}}$ replaces $m^{*3/2}$ of Eq. (5.6). One therefore defines a density of states mass m_d

$$m_d^* = (m_l^* m_t^{*2})^{1/3} \tag{5.12}$$

which differs from the conductivity mass of Eq. (3.31).

Higher in the conduction band, the proportionality of $g(E)$ to $\sqrt{E - E_c}$ ceases to be true because of the complicated $E(\mathbf{k})$ relation for the conduction band of semiconductors such as silicon or gallium arsenide (Figure 5.2). In this case the density of states cannot be calculated explicitly but is easily calculated by numerical methods. To understand these methods, consider a surface of constant energy E_0 in **k** space. This surface is equal to the circle shown in Figure 5.1 only for the simple case of isotrospic effective mass. In general this will be a surface (two-dimensional in three-dimensional **k** space) of arbitrary complicated shape. We now could calculate the number of states in the volume of this surface similar to Eqs. (5.3) and (5.4). However, we also can directly look at the number of states in the differential volume between the surface E_0 and $E_0 + dE$. The thickness dE expressed in terms of $\mathbf{k}_\perp$ (the unit vector perpendicular to the equal average surface) reads:

$$dE = |\nabla_{\mathbf{k}} E(\mathbf{k})| d\mathbf{k}_\perp \tag{5.13}$$

as known from calculus, and therefore the density of states is given by

$$g(E_0) = \int \frac{ds}{|\nabla_{\mathbf{k}} E(\mathbf{k})|} \tag{5.14}$$

Here ds signifies the surface integral over the surface of equal energy E_0 in **k** space. This integral can be evaluated by very efficient numerical methods.

The integration is performed by selecting a random sequence of points $\mathbf{k}_j$ within the first Brillouin zone around which differential contributions to the density of states are calculated. Within a small fixed-size radius R_s of each point $\mathbf{k}_j$, $E(\mathbf{k})$ is assumed to be a linear function of **k**. $E(\mathbf{k}_j)$ and $\nabla E_k(\mathbf{k}_j)$ are evaluated. If part of a surface $E(\mathbf{k}) = E_0$ lies within the small sphere of radius R_s centered at $\mathbf{k}_j$, the shortest distance between this surface and $\mathbf{k}_j$ is $R_e = |(E_0 - E(\mathbf{k}_j))/\nabla_k E(\mathbf{k}_j)|$. Therefore, the area of intersection between this surface and the small sphere is $\pi(R_s^2 - R_e^2)$, and its contribution to the density of states is simply $\pi(R_s^2 - R_e^2)/|\nabla_k E(\mathbf{k}_j)|$. This procedure is iterated until the desired accuracy is reached, taking care to normalize $g(E)$ appropriately with the number of points selected.

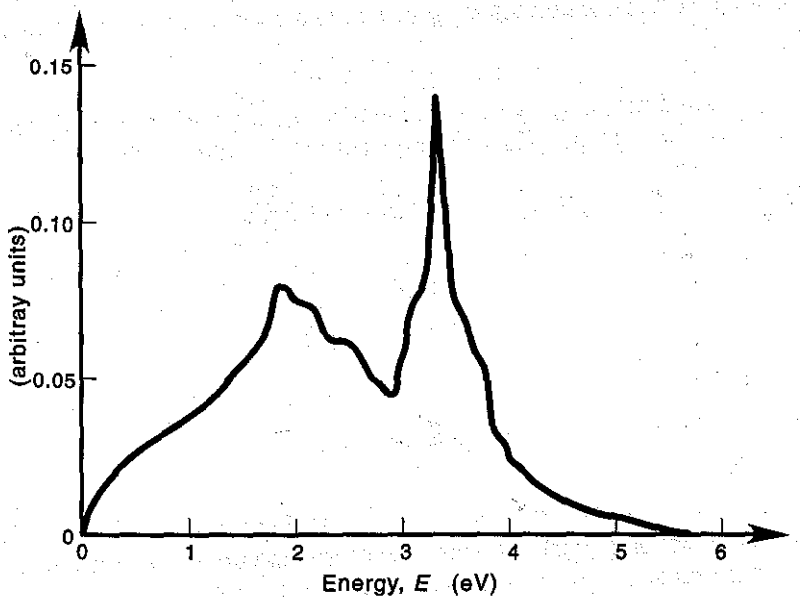

Figure 5.2 The density of states for silicon as calculated from the empirical pseudopotential model (conduction band).

These modifications of the explicit simple treatment of the density of states are necessitated by the complicated form of the energy bands at high energies far above (below) the band edges. Also, at low energies, modifications of the proportionality of $g(E)$ to $\sqrt{E - E_c}$ can be important. These modifications are usually a consequence of the doping. Figure 5.3 shows the impurity-related density of states for various degrees of doping. For light doping (Figure 5.3a), the impurity levels are the single "hydrogen-like" levels. For higher impurity densities (Figure 5.3b), an impurity band develops that merges at very high concentrations with the conduction band (Figure 5.3c). In the latter case, the semiconductor behaves as a metal; that is, it is highly conducting down to the lowest temperatures.

A simple semiquantitative treatment of the impurity "band tail," shown in Figure 5.3c, has been proposed by Kane [2]. His treatment rests on the assumption of a local conservation of the density of states. He visualizes the impurity potential at high impurity densities as a smoothly varying potential $V_I(\mathbf{r})$, as shown in Figure 5.4.

The density of states at each point **r** is the density of states of the unperturbed crystal as shown in Figure 5.4. In other words, the conduction band edge is locally shifted and the density of states starts to increase from these shifted energy values. The fact that the conduction band edge is shifted exactly as the potential $V_I(\mathbf{r})$ follows, of course, from the effective mass theorem, which is then the basis of Kane's theory.

Kane further suggests using the potential $V_I(r)$ as a stochastic variable obey-

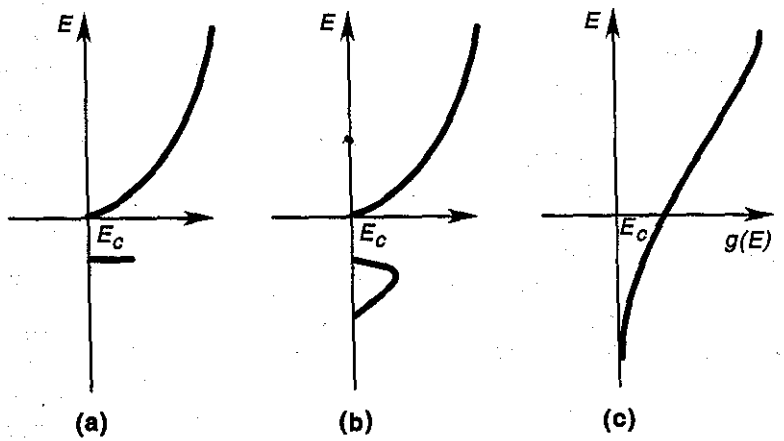

Figure 5.3 Density of states in a semiconductor including impurity levels.

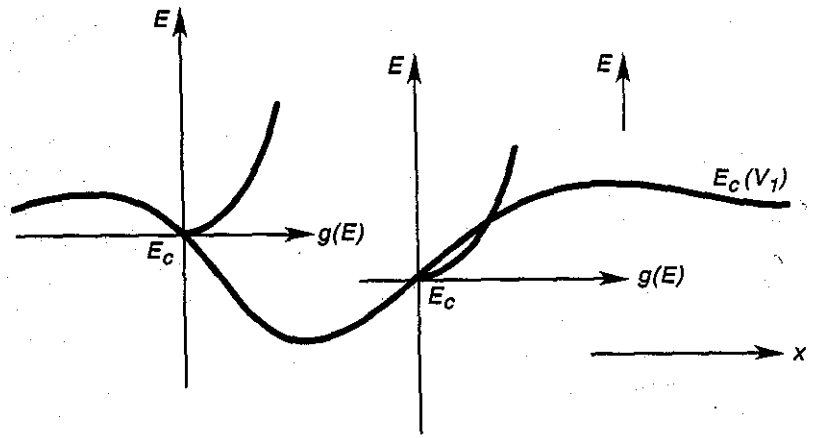

Figure 5.4 The locally conserved density of states in a slowly varying potential of impurities.

ing a Gaussian distribution F

$$F(V_I) = \frac{1}{\sqrt{\pi}} \exp(-e^2 V_I^2/\eta^2) \tag{5.15}$$

The quantity η has been also estimated by Kane [2]. For our purposes, it is sufficient to regard it as parameter (a typical value for 10^{19} cm^{-3} impurities would be 50 meV). If the unperturbed density of states is denoted by $g(E)$ and the density of states including impurities by $g_I(E)$, we obtain

$$g_I(E) = \int_{-\infty}^{E-E_c} g(E - eV_I) F(eV_I)\, d(eV_I) \tag{5.16}$$

The equation is general enough to hold also for two-dimensional systems. Remember, however, that Eq. (5.16) is based on the effective mass theorem and will

fail for very close spacing of impurities.

A very different treatment, valid for the "deeper" band tail, has been given by Halperin and Lax [1]. Although this theory does not rely on the simple picture of the effective mass approach, it is valid only in the deeper band tail and is not simple enough for engineering applications. We therefore propose a pragmatic approach for complex simulations related to devices: use Eq. (5.16) and evaluate η from pertinent experimental data for the (restricted) range of doping densities that is of interest.

5.2 PROBABILITY OF FINDING ELECTRONS IN A STATE

Here we describe equilibrium statistics, which are well known and described in many other texts. We therefore list only a few facts that are used in the following and refer the reader for derivation to the excellent treatment by Landsberg [3].

In equilibrium, the probability of finding an electron in a state of energy E is given by the Fermi distribution f, as derived in texts of statistical mechanics

$$f(E) = \frac{1}{e^{(E-E_F)/kT} + 1} \tag{5.17}$$

The parameter E_F is known as the Fermi level (chemical potential) and is determined by the total number of charge carriers.

Figure 5.5 shows $f(E)$ for $T = 0$ and $T \neq 0$. For zero temperature, $f(E) = 1$ below E_F and $f(E) = 0$ above E_F . This means that all the states below E_F will be filled and all above it will be empty if $T = 0$. For higher temperatures, the distribution function exhibits an exponential (Maxwell-Boltzmann) tail.

There are two important approximations to $f(E)$. For low temperatures, $f(E)$ can be approximated by the step function $H(E - E_F)$, as evident from Figure 5.5.

$$f(E)_{T\sim 0} \approx H(E - E_F) \tag{5.18}$$

In this case, the derivative of f is

$$\frac{\partial f(E)}{\partial E} = -\delta(E - E_F) \tag{5.19}$$

A general useful relation is also

$$\frac{\partial f(E)}{\partial E} = -f(E)(1 - f(E))/kT \tag{5.20}$$

If we are only interested in the higher energy tail of $f(E)$, then we can neglect the one compared to the exponent in Eq. (5.17), which gives

$$f(E) \approx e^{(E_F - E)/kT} \tag{5.21}$$

Remember that at finite temperatures E_F is the parameter that characterizes the density of electrons [see Eq. (5.23)] and represents the ch[illegible]al potential,

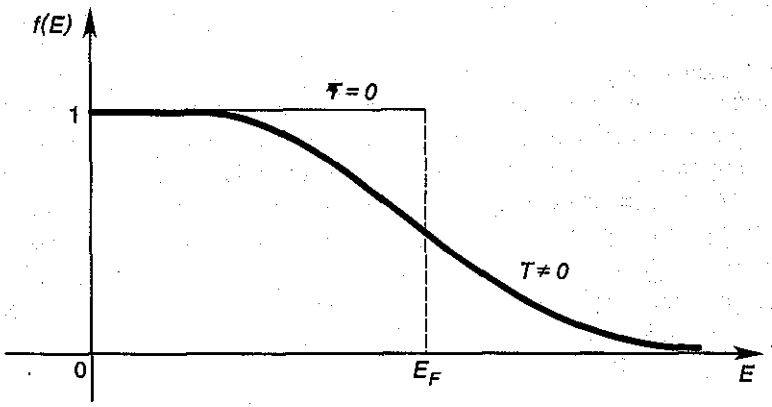

Figure 5.5 Fermi distribution as function of energy.

which is temperature dependent itself. The function of Eq. (5.21) is called the Maxwell-Boltzmann distribution function.

Holes like electrons obey Fermi statistics, but as if their energy were measured "downwards." This can easily be seen from the fact that the hole distribution f_h equals $1-f$, where f is the electron distribution.

Equation (5.21) describes the probability of finding an electron in a conduction band state of energy E. Remember that two electrons of opposite spin can occupy such a state. This factor of two is included in our treatment of the density of states. The probability that the energy level of a donor is occupied is more difficult to calculate for various reasons. For one, a donor can usually only accommodate one electron (the one which is then "donated"). There are, however, in addition to the ground state, excited states available for the electron and the various states with and without the electron can have degeneracies (e.g., owing to the fact that two spin states are available to the electron bound by the donor). As a consequence one obtains for the probability $f_{D/A}$ of occupation for a donor/acceptor of energy $E_{D/A}$:

$$f_{D/A} = \frac{1}{1+\beta_{D/A}\exp(E_{D/A}-E_F)/kT} \tag{5.22}$$

where the factor $\beta_{D/A}$ can often be approximated by $\beta_D = 1/2$ and $\beta_A = 2$ as derived in Landsberg's [3] treatment. Note that the establishment of such a distribution depends on the communication of the donors with band states and can take considerable time as discussed in Chapter 9.

5.3 ELECTRON DENSITY IN THE CONDUCTION BAND

From Eq. (5.7), by using Eq. (5.22) for the distribution function (which will be justified below), we obtain for the density n in the conduction band

$$n_c = \frac{1}{2\pi^2}\left(\frac{2m^*}{\hbar^2}\right)^{3/2}\int_0^\infty (1+\exp(E-E_F)/kT)^{-1}\sqrt{E}\,dE \tag{5.23}$$

Here we have assumed that the conduction band extends toward infinity (the exponent decays rapidly) and we have chosen the conduction band edge as the zero of the energy. Note, also, that an effective mass of a single minimum has been used. Substituting $\bar{x}$ for E/kT and $\bar{x}_F$ for E_F/kT. One is left with a Fermi integral defined by

$$I_{\frac{1}{2}}(\bar{x}_F) = \frac{2}{\sqrt{\pi}}\int_0^\infty \frac{\bar{x}^{1/2}}{1+\exp(\bar{x}-\bar{x}_F)}\,d\bar{x} \tag{5.24}$$

which must be evaluated to obtain the carrier concentration n_c in the conduction band. For $\bar{x}_F < -2$, the exponent in the denominator of Eq. (5.24) dominates and, if one seeks accuracy within a few percent only, the one can be neglected. The integral then becomes equal to the Γ function.

$$\int_0^\infty e^{-\bar{x}}\bar{x}^s d\bar{x} = \Gamma(s+1) \tag{5.25}$$

and we obtain

$$n_c = \frac{1}{4}\left(\frac{2m^*kT}{\pi\hbar^2}\right)^{3/2} e^{E_F/kT} \equiv N_c e^{E_F/kT} \tag{5.26}$$

where N_c is called the effective density of states for the conduction band. Here we have used the following expression for the Γ function:

$$\Gamma(1/2) = \sqrt{(\pi)} \tag{5.27}$$

and

$$\Gamma(s+1) = s\Gamma(s) \tag{5.28}$$

which is valid for s being an integer multiple of $1/2$. For s being integer, we simply have

$$\Gamma(s+1) = s! \tag{5.29}$$

For the density p of holes in the valence band, we obtain in a similar manner

$$p = \frac{1}{4}\left(\frac{2m_h^*kT}{\pi\hbar^2}\right)^{3/2} e^{(-E_G-E_F/kT)} \equiv N_v e^{(-E_G-E_F)/kT} \tag{5.30}$$

where E_G is the band gap energy.

One usually defines an "intrinsic concentration" n_i by the product $n \cdot p$. This product is given by

$$n_i^2 = n \cdot p = \frac{1}{2}\left(\frac{kT}{\pi\hbar^2}\right)^3 (m_n^* m_h^*)^{3/2} e^{-E_G/kT} \equiv N_c N_v e^{-E_G/kT} \tag{5.31}$$

As can be seen, this product depends only on semiconductor material parameters and not on the Fermi energy. Equation (5.31), therefore, holds also when the semiconductor is doped. Of course, if the doping goes up to levels so that $\bar{x}_F < -2$, the approximations are invalid and so is Eq. (5.31). In this case the integrals $I_{1/2}(\bar{x}_F)$ appear in the final result. Note, however, that even these integrals are correct only if the density of states is proportional to the square root of the energy. For the general case of Eq. (5.16), $I_{1/2}(\bar{x}_F)$ is replaced by a more general integral

$$I_{g(\bar{x})}(\bar{x}_p) \propto \int_0^\infty \frac{g_I(\bar{x})}{1+\exp(\bar{x}-\bar{x}_F)}\, d\bar{x} \tag{5.32}$$

where $g_I(\bar{x})$ can be calculated by (numerical) integration from Eq. (5.16) and represents the energy dependence of the density of states that replaces $\sqrt{\bar{x}}$. To determine the electron and hole concentration in a given band we still need to determine the Fermi level E. The Fermi level E_F can be calculated from the charge neutrality condition. For the pure semiconductor this condition means

$$p = n \tag{5.33}$$

and both n and p (now termed the intrinsic concentrations n_i, p_i) can be calculated from Eq. (5.31).

In the presence of charged donors, of constant density N_D^+, and charged acceptors, of constant density N_A^-, charge neutrality must be written as

$$N_D^+ + p = N_A^- + n \tag{5.34}$$

To solve Eq. (5.34) for the Fermi level, we need to express N_D^+ and N_A^- as a function of E_F. The total density N_D of donors (or of acceptors N_A) can often be assumed as given, as for example deduced from the method of doping (diffusion, ion implantation). The density of charged donors N_D^+ (or acceptors N_A^-) is then obtained by mulitiplying the total density with the probability for a donor to be empty or acceptor to be filled, which can be obtained from Eq. (5.22). Equation (5.34) therefore represents, in general, a transcendental equation for E_F. If band tailing is included, the equation may in addition contain numerical double integrations involving Eq. (5.16) and Eq. (5.32). Nevertheless, such equations are easy to solve with current personal computers by use of the Newton method (see, e.g., *Numerical Recipes* [4]).

To remind the reader of the most important special cases, we add here a few analytical considerations:

1. The pure semiconductor with $m^* = m_h^*$. In this case, the equation of charge neutrality, Eq. (5.33), together with Eq. (5.26) and Eq. (5.30), gives

$$E_F = -E_G/2 \tag{5.35}$$

That is, the Fermi energy is in the middle of the energy gap (if $m_h^* \neq m^*$, it will be slightly shifted). This justifies *a posteriori* the use of the Maxwellian distribution for the calculation of n_c because only the tail of the distribution function is within the conduction band. The intrinsic concentration of several semiconductors is shown in Figure 5.6.

2. A semiconductor is doped with N_D donors and $N_D \gg n_i$. Furthermore, we assume that at high temperatures $N_D \approx N_D^+$, while at low temperatures $N_D^+ = 0$ (the electrons "freeze out" back to their parent donors, as shown below). Then

$$n = \frac{n_i^2}{n} + N_D \approx N_D \tag{5.36}$$

for high temperatures, while $n \approx 0$ for low temperatures. Notice, however, that if the temperature becomes very high, the term n_i^2/n in Eq. (5.36) cannot be neglected as the intrinsic concentration rises. This gives the graph n versus T, as shown in Figure 5.7.

3. At low temperataures, the assumption $N_D \approx N_D^+$ does not hold because the thermally excited electrons recombine with the donors largely neutralizing them. N_D^+ is generally given by

$$N_D^+ = N_D(1 - f_D) \tag{5.37}$$

with f_D from Eq. (5.22).

Equation (5.34) then reads in the absence of acceptors

$$N_D(1 - f_D) + p = n \tag{5.38}$$

In the limit $T \to 0K$, f_D approaches one and all terms in Eq (5.38) approach zero. Physically the electrons "freeze out" from the conduction band and recombine with their "parent" donors.

It is easy to include the ellipsoidal shape of the equal energy surfaces in our calculations. For example, if we consider the silicon conduction band, we have to replace m_n^* by $(m_l^* m_t^{*2})^{1/3}$ and multiply the result by 6 because we have six degenerate ellipsoids located inside the Brillouin zone. Germanium has eight ellipsoids whose center is at the L point of the Brillouin zone. Within the zone there is only one-half of each ellipsoid and we have to multiply the result by a factor of 4 instead of by 6, as in the case of silicon.

Let us finally mention that another complication in the calculation of carrier densities arises from the fact that the energy gap E_G actually depends on temperature. There are different reasons for this temperature dependence, which are

Gang Chen
"Nanoscale Energy Transport and Conversion"
Oxford (2005)

4.1.4 Fermi–Dirac, Bose–Einstein, and Boltzmann Distributions

Let's now consider the probability of electrons occupying a specific quantum state. We assume that we have determined the accessible quantum states for electrons in a given system. From the Pauli exclusion principle, each quantum state can have a maximum of one electron. If the system is at equilibrium with a temperature T, we wish to determine the probability of one quantum state having energy E being empty or occupied by one electron. We take this specific quantum state as our system, and the rest of the accessible quantum states of the original system are grouped into the reservoir. There can be energy and particle exchanges between the new system and its reservoir because an electron can fluctuate randomly between this quantum state and other quantum states. Thus the

appropriate ensemble for the new system is the grand canonical ensemble. The grand canonical partition function for the new system can be evaluated from eq. (4.18),

$$\Im(T, V, \mu) = \sum_{N_i=0}^{1} \gamma^{N_i} Z_i = 1 + \exp\left(\frac{\mu - E}{\kappa_B T}\right) \tag{4.35}$$

where $N_i = 0$ means that the quantum state is unoccupied, with system energy at zero, and $N_i = 1$ means that the state is occupied, with system energy at E. According to eq. (4.17), the probability that this quantum state is empty or occupied is, respectively,

$$P(E_i = 0, N_i = 0) = P_0 = \frac{1}{1 + \exp\left(\frac{\mu - E}{\kappa_B T}\right)} \quad \text{(empty)} \tag{4.36}$$

and

$$P(E_i = E, N_i = 1) = P_1 = \frac{\exp\left(\frac{\mu - E}{\kappa_B T}\right)}{1 + \exp\left(\frac{\mu - E}{\kappa_B T}\right)} \quad \text{(occupied)} \tag{4.37}$$

The average number of occupancy of this quantum state is thus

$$\begin{aligned} \langle n \rangle \equiv f(E) &= 0 \times P(E_i = 0, N_i = 0) + 1 \times P(E_i = E, N_i = 1) \\ &= \frac{1}{\exp\left(\frac{E - \mu}{\kappa_B T}\right) + 1} \end{aligned} \tag{4.38}$$

and the average energy of this quantum state is

$$\begin{aligned} \langle E \rangle &= 0 \times P(E_i = 0, N_i = 0) + E \times P(E_i = E, N_i = 1) \\ &= \frac{E}{\exp\left(\frac{E - \mu}{\kappa_B T}\right) + 1} = Ef(E) \end{aligned} \tag{4.39}$$

$\langle n \rangle$, or in a more popular symbol f, is called the *Fermi–Dirac distribution function.* Electrons and other particles that obey the Fermi–Dirac distributions are called *fermions.* Figure 4.3 illustrates this distribution function. Recall that μ is the chemical potential. When the energy is a few times of $\kappa_B T$ smaller than the chemical potential, the distribution is close to one, indicating that most of the energy states below the chemical potential are occupied. When the energy is a few times of $\kappa_B T$ larger than the chemical potential, the distribution function is close to zero, indicating that most states above the chemical potential are empty. Because the motion of electrons means that there must be unoccupied states for the electrons to fill, only the electrons close to the chemical potential are active in carrying the charge. At zero temperature, the chemical potential equals the Fermi level. In some fields, however, particularly electrical engineering, the chemical potential and the Fermi level are used interchangeably.

Next, let's consider the probability of phonons or photons occupying an accessible quantum state of the system. Unlike electrons, the number of phonons or photons in a system is not conserved. Thus N is not a thermodynamic variable for the system,

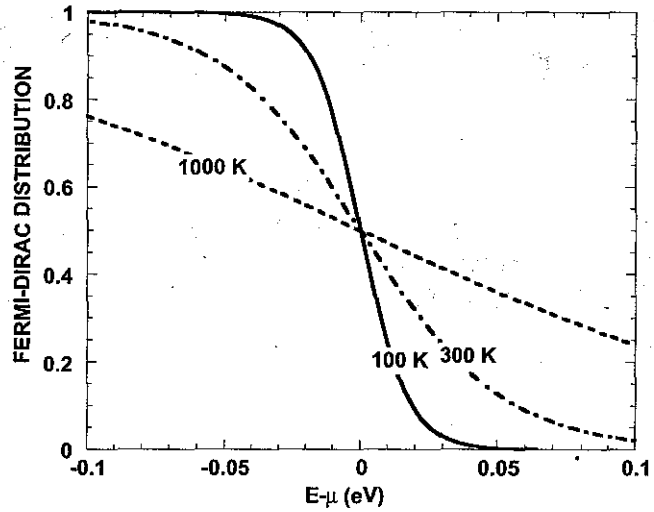

Figure 4.3 Fermi–Dirac distribution as a function of the electron energy relative to the chemical potential.

and, correspondingly, neither is the chemical potential. We know that for an accessible quantum state of the system, with frequency ν, there can be an arbitrary number n of photons or phonons such that the total energy of this state is $E = (n + 1/2)h\nu$ ($n = 0, 1, 2, \ldots$). Following a similar argument as for electrons, we take this quantum state to be our new system and the remaining quantum states to be the reservoir. Since neither the chemical potential nor the particle number is a thermodynamic variable, the new system is best described by a canonical ensemble with the canonical partition function

$$Z(\nu) = \sum_{n=0}^{\infty} \exp\left(-\frac{(n+1/2)\,h\nu}{\kappa_B T}\right) = \frac{\exp\left(-\frac{h\nu}{2\kappa_B T}\right)}{1 - \exp\left(-\frac{h\nu}{\kappa_B T}\right)} \tag{4.40}$$

The probability that the quantum state (the new system) has n particles (photons or phonons) is thus

$$P(\nu, n) = \frac{\exp\left(-\frac{(n+1/2)h\nu}{\kappa_B T}\right)}{Z} = \exp\left(-\frac{nh\nu}{\kappa_B T}\right)\left[1 - \exp\left(-\frac{h\nu}{\kappa_B T}\right)\right] \tag{4.41}$$

and the average number of the particles, or the occupancy of the quantum state, is

$$\langle n \rangle \equiv f(\nu) = \sum_{n=0}^{\infty} nP(\nu, n) = \frac{1}{\exp\left(\frac{h\nu}{\kappa_B T}\right) - 1} \tag{4.42}$$

This equation is the *Bose–Einstein distribution function*, and the particles obeying this distribution are called *bosons*. Figure 4.4 shows the Bose–Einstein distribution. Because each particle has energy $h\nu$, the average energy of the quantum state is

$$\langle E \rangle = h\nu f(\nu) \tag{4.43}$$

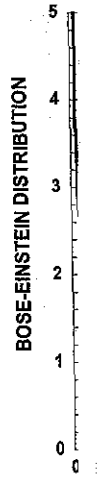

Figure 4.4 Bose–Ein
photons).

where we have neg
transfer processes.

Other boson syst
For such bosons, w
general Bose–Einst

where μ is again th

The Bose–Einst
Fermi–Dirac distril
and high temperatu
Boltzmann distribu

$f(E,$

This distribution fu
Einstein distributic
between "classical'

4.2 Inte

The statistical dis
quantum state and

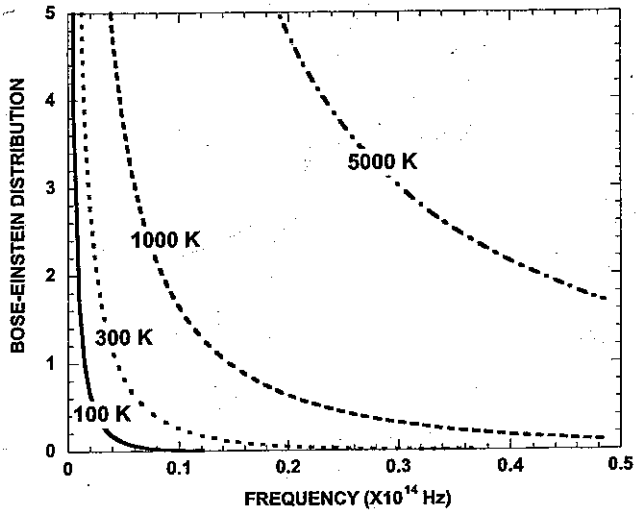

Figure 4.4 Bose–Einstein distribution as a function of the frequency of the carriers (phonons and photons).

where we have neglected the zero-point energy, which does not participate in heat transfer processes.

Other boson systems, such as gas molecules, can have a fixed number of particles. For such bosons, we should use the grand canonical ensemble as for fermions, and the general Bose–Einstein distribution can be written as

$$\langle n \rangle \equiv f(E) = \frac{1}{\exp\left(\frac{E-\mu}{\kappa_B T}\right) - 1} \tag{4.44}$$

where μ is again the chemical potential of the boson gas.

The Bose–Einstein distribution changes the "plus one" in the denominator of the Fermi–Dirac distribution into minus one. In the limit of low occupancy (high energy and high temperature), both Bose–Einstein and Fermi–Dirac distributions reduce to the Boltzmann distribution function

$$f(E, T, \mu) = \exp\left(-\frac{E-\mu}{\kappa_B T}\right) \text{ or } f(E) = \exp\left(-\frac{E}{\kappa_B T}\right) \tag{4.45}$$

This distribution function is considered as "classical", while the Fermi–Dirac and Bose–Einstein distributions are "quantum." Thus, for the statistical distributions, difference between "classical" and "quantum" statistics lies merely in the "one" of the denominator!

4.2 Internal Energy and Specific Heat

The statistical distribution functions establish a link with temperature between the quantum state and its energy level. With the distribution functions, we can investigate

the properties of matter at finite temperatures. In this section we consider the internal energy and specific heat. Recall that the constant volume specific heat per unit volume, C_V [J m^{-3} K^{-1}], is defined as

$$C_V = \frac{1}{V}\left(\frac{\partial U}{\partial T}\right)_V \tag{4.46}$$

where U is the average internal energy of the system. We will consider the internal energy and specific heat of various energy carriers in this section.

4.2.1 Gases

For a dilute monatomic gas, the total internal energy is given by eq. (4.30). Consequently, the volumetric specific heat is

$$C_V = \frac{1}{V}\frac{3}{2}\kappa_B N \tag{4.47}$$

Since the number of molecules per mole equals Avogadro's constant $N_A = 6.02 \times 10^{23}$ mol^{-1}, the specific heat per mole for a monatomic gas is

$$c_V = \frac{3}{2}\kappa_B N_A = \frac{3}{2}R \tag{4.48}$$

where $R(= \kappa_B N_A = 8.314\ \text{J K}^{-1}\ \text{mol}^{-1})$ is the universal gas constant.

For a diatomic gas, we should consider the contributions from the rotational and vibrational states. We already have from eq. (E.4.1.3) the rotational partition function of one diatomic molecule,

$$Z_r = \sum_{l=0}^{\infty}(2\ell+1)\exp\left[-\frac{\theta_r \ell(\ell+1)}{T}\right] \tag{4.49}$$

We will consider next the vibrational partition function. The vibrational energy of a harmonic oscillator was derived in chapter 2 as

$$E = h\nu\left(n+\frac{1}{2}\right) \quad (n = 0, 1, 2, \ldots) \tag{4.50}$$

The vibrational partition function is thus

$$Z_v = \sum_{n=0}^{\infty}\exp\left(-\frac{h\nu(n+1/2)}{\kappa_B T}\right) = \frac{\exp\left(-\frac{\theta_v}{2T}\right)}{\exp\left(\frac{\theta_v}{T}\right)-1} \tag{4.51}$$

where $\theta_v = h\nu/\kappa_B$ is called the vibrational temperature.

In addition, the molecule also has electronic energy states. From the solution of the electronic energy levels in chapter 2 for a hydrogen atom, we know that the electronic

energy levels are high and that their separations are large. So we can take the first term only of the electronic partition function

$$Z_e = g_{e1}\exp\left[-\frac{E_{e1}}{\kappa_B T}\right] + g_{e2}\exp\left[-\frac{E_{e2}}{\kappa_B T}\right] + \cdots \approx g_{e1}\exp\left[-\frac{E_{e1}}{\kappa_B T}\right] \tag{4.52}$$

where E_{ei} is the ith electronic energy level and g_{ei} is the degeneracy for that energy level. From eqs. (4.27) and (4.32), the canonical partition function for N molecules is

$$Z_N = \frac{(Z_t Z_r Z_v Z_e)^N}{N!} \tag{4.53}$$

and the average internal energy of the molecule, according to eq. (4.30), is thus

$$\begin{aligned} U &= \kappa_B T^2 \frac{\partial}{\partial T}\left\{\ln\left(\frac{(Z_t Z_r Z_v Z_e)^N}{N!}\right)\right\} \\ &= \kappa_B T^2 N\left\{\frac{\partial}{\partial T}(\ln Z_t) + \frac{\partial}{\partial T}(\ln Z_r) + \frac{\partial}{\partial T}(\ln Z_v)\right. \\ &\quad \left. + \frac{\partial}{\partial T}(\ln Z_e) - (\ln N - 1)\right\} \end{aligned} \tag{4.54}$$

The volumetric specific heat can be obtained by taking the derivative of U with respect to T at constant V. The translational energy contribution to the specific heat is given by eq. (4.47). The electronic energy level contribution to the specific heat is

$$C_{V,e} = \frac{N}{V}\frac{\partial}{\partial T}\left[\kappa_B T^2 \frac{\partial}{\partial T}\ln Z_e\right] = 0 \tag{4.55}$$

This result is because the electrons are only sitting in the first energy states and their contribution to the total system energy does not change with temperature. The contribution of rotational energy states to specific heat is

$$C_{V,r} = \frac{N}{V}\frac{\partial}{\partial T}\left[\kappa_B T^2 \frac{\partial}{\partial T}\ln\left(\sum_{\ell=0}^{\infty}(2l+1)\exp\left[-\frac{\theta_r \ell(\ell+1)}{T}\right]\right)\right] \tag{4.56}$$

We know, from eq. (E4.1.3), that the summation in the above equation is proportional to T/θ_r at high temperatures. In this limit, the contribution of the rotational energy level to the specific heat is

$$C_{V,r} = N\kappa_B/V \text{(at high temperature)} \tag{4.57}$$

This result is again a manifestation of the equipartition theorem. A diatomic molecule has two degrees of rotational freedom. So at high temperatures, when the rotational levels are fully excited, each molecule contributes $2 \times \kappa_B T/2 = \kappa_B T$ to the average

energy. At low temperatures, the rotational specific heat must be calculated from the full rotational partition function in the summation format, eq. (4.56). Similarly, the contribution of the vibrational energy state to the specific heat is

$$C_{V,v} = \frac{\kappa_B N}{V} \frac{\theta_v^2}{T^2} \frac{e^{\theta_v/T}}{(e^{\theta_v/T}-1)^2} \tag{4.58}$$

At high temperatures, the above formula leads to

$$C_{V,v} \approx \frac{\kappa_B N}{V} \tag{4.59}$$

which is again a manifestation of the equipartition theorem. After obtaining the contributions from all the energy modes, we calculate the total specific heat of a diatomic molecule by summing each of the contributing terms: $C_V = C_{V,t} + C_{V,r} + C_{V,v} + C_{V,e}$. The following example shows more numerical details.

Example 4.2 *Specific heat of* H_2

The rotational temperature of a hydrogen molecule is 85.3 K and its vibrational temperature is 6332 K. Plot the specific heat of hydrogen gas as a function of temperature.

Solution: From eqs. (4.48), (4.56), and (4.58), we can write the total specific heat per mole of a diatomic gas as

$$\frac{c_V}{R} = \frac{3}{2} + \left(\frac{\theta_v}{T}\right)^2 \frac{e^{\theta_v/T}}{(e^{\theta_v/T}-1)^2} + \frac{\partial}{\partial T}\left[T^2 \frac{\partial}{\partial T} \ln\left(\sum_\ell (2\ell+1)\exp\left[-\frac{\theta_r \ell(\ell+1)}{T}\right]\right)\right] \tag{E4.2.1}$$

The last term in the above equation can be written as

$$\frac{c_{V,r}}{R} = \left(\frac{\theta_r}{T}\right)^2 \times \frac{Z_r \sum_\ell (2\ell+1)\ell^2(\ell+1)^2 \exp\left[-\frac{\theta_r \ell(\ell+1)}{T}\right] - \left\{\sum_\ell (2\ell+1)\ell(\ell+1)\exp\left[-\frac{\theta_r \ell(\ell+1)}{T}\right]\right\}^2}{Z_r^2} \tag{E4.2.2}$$

A computer program is used to carry out the above summation. Figure E4.2 plots the variation of c_V/R with temperature. At low temperatures, only the translational energy levels are fully excited and the specific heat is $3R/2$. As the temperature increases, the rotational energy levels become excited and contribute to the specific heat up to a maximum of R so that the total specific heat reaches $5R/2$. At even higher temperatures, the vibrational energy levels start contributing to the specific heat, which approaches a final value of $7R/2$.

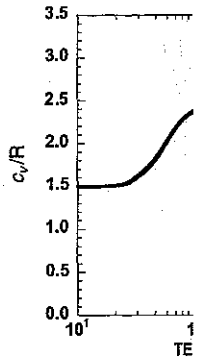

4.2.2 El

Now we investiga
have a parabolic l

We obtained the

The total number

From eq. (4.62), t
for a given n. For

We have alread
μ at $T = 0$ is cal
explicitly integrat
can use the Boltzr
Equation (4.62) c

$$n = \int_{E_c}^{\infty} \exp\left(-\right.$$

*In electronics, hc

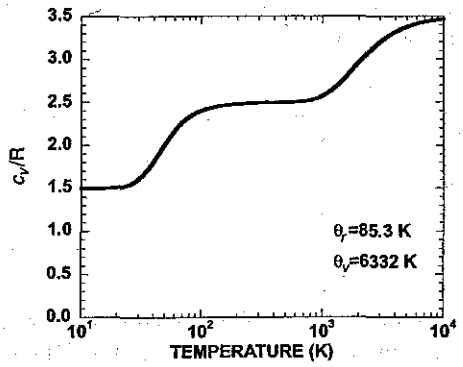

Figure E4.2 Specific heat of H_2 gas as a function of temperature.

4.2.2 Electrons in Crystals

Now we investigate the specific heat of electrons in a crystal. We assume that the electrons have a parabolic band with an isotropic effective mass

$$E - E_c = \frac{\hbar^2}{2m^*}(k_x^2 + k_y^2 + k_z^2) \tag{4.60}$$

We obtained the density of states in chapter 3, eq. (3.52),

$$D(E) = \frac{1}{2\pi^2}\left(\frac{2m^*}{\hbar^2}\right)^{3/2}(E - E_c)^{1/2} \tag{4.61}$$

The total number of electrons per unit volume is thus

$$n = \int_0^\infty f(E, T, \mu)D(E)\,dE \tag{4.62}$$

From eq. (4.62), the chemical potential as a function of temperature can be determined for a given n. For $T = 0$, the above relation leads to

$$n = \int_{E_c}^{\mu} D(E)\,dE = \frac{1}{3\pi^2}\left(\frac{2m^*}{\hbar^2}\right)^{3/2}(\mu - E_c)^{3/2} \tag{4.63}$$

We have already obtained this relation, eq. (3.53), in chapter 3. The chemical potential μ at $T = 0$ is called the Fermi level, E_f.* At other temperatures, eq. (4.62) cannot be explicitly integrated. However, when $(E-\mu)/k_BT \gg 1$, which is the classical limit, we can use the Boltzmann distribution as an approximation of the Fermi–Dirac distribution. Equation (4.62) can be integrated explicitly,

$$n = \int_{E_c}^{\infty} \exp\left(\frac{-E+\mu}{\kappa_B T}\right)\frac{1}{2\pi^2}\left(\frac{2m^*}{\hbar^2}\right)^{3/2}(E - E_c)^{1/2}\,dE = N_c \exp\left(-\frac{E_c - \mu}{\kappa_B T}\right) \tag{4.64}$$

*In electronics, however, E_f is often used to represent the chemical potential at all temperatures.

with

$$N_c = 2\left(\frac{2\pi m^* \kappa_B T}{h^2}\right)^{3/2} \tag{4.65}$$

Equation (4.64) is often used to determine the chemical potential level in doped semiconductors, as will be seen from the following example.

Example 4.3 *Chemical potential level in doped semiconductors*

Silicon is a widely used semiconductor material, and it is often doped with phosphorus to form an n-type semiconductor. Determine the chemical potential of an n-type semiconductor doped with phosphorus with a concentration of 10^{17} cm^{-3} at 300 K, assuming that every phosphorus atom contributes one free electron to the conduction band and neglecting thermally excited electrons from the valence band. Although the silicon conduction bands are not spherical [figure 3.18(b)], they can be approximated by an isotropic band with an effective mass equal to $0.33m$, where m is the free electron mass.

Solution: Silicon has six identical conduction bands [figure 3.18(b)]. When counting all six bands, eq. (4.64) should be written as

$$n = 12\left(\frac{2\pi m * \kappa_B T}{h^2}\right)^{3/2} \exp\left(-\frac{E_c - \mu}{\kappa_B T}\right) \tag{E4.3.1}$$

Taking $n = 10^{17}$ cm^{-3}, we can find the chemical potential as

$$\begin{aligned}\frac{\mu - E_c}{\kappa_B T} &= \ln\left[\frac{n}{12}\left(\frac{2\pi m^* \kappa_B T}{h^2}\right)^{-3/2}\right] \\ &= \ln\left[\frac{10^{23}}{12}\left(\frac{2\pi \times 0.33 \times 9.1 \times 10^{-31} \times 1.38 \times 10^{-23} \times 300}{6.6^2 \times 10^{-68}}\right)^{-3/2}\right] \\ &= -5.65 \end{aligned} \tag{E4.3.2}$$

Thus

$$\mu - E_c = -5.65 \times 26 \text{ meV} = -147 \text{ meV} \tag{E4.3.3}$$

Comments. 1. The negative sign means that the chemical potential is below the conduction band edge. The silicon bandgap at room temperature is 1.12 eV. Thus the chemical potential level is within the bandgap. In fact, only in this case, the Boltzmann approximation we used in eq. (4.64) is applicable because the electron energy inside the conduction band, minus the chemical potential, is much larger than $\kappa_B T$. If the chemical potential is close to the band edge or falls

inside the conduction band, which is the case when the semiconductors are heavily doped, we need to carry out numerical integration with the Fermi–Dirac statistical distribution.

2. The value of the chemical potential needs a reference point. Equation (4.64) suggests that it is the relative difference between μ and E_c that determines the electron number density, and thus this difference is the value of the chemical potential. In chapter 6 (figure 6.9), we will give a more detailed discussion on the reference point issue.

To calculate the specific heat of electrons, we first formulate the internal energy of electrons as

$$U(T) = \int_{E_c}^{\infty} EF(E, T, \mu)D(E)dE \tag{4.66}$$

For convenience, we limit our discussion to metals so that the number of electrons per unit volume n_e is fixed. We further take $E_c = 0$ as reference, eq. (4.62) becomes

$$n_e = \int_{0}^{\infty} f(E, T, \mu)D(E)dE = \text{constant} \tag{4.67}$$

We can use eq. (4.67) to rewrite eq. (4.66) as

$$U(T) = \int_{0}^{\infty} (E - E_f)f(E, T, \mu)D(E)dE + E_f n_e \tag{4.68}$$

where E_f is the Fermi level (μ at $T = 0$ K). In eq. (4.68), since only f is temperature dependent, we obtain the heat capacity of the electron system as

$$C_e = \int_{0}^{\infty} (E - E_f)\frac{df(E, T, \mu)}{dT}D(E)dE \tag{4.69}$$

Typically, df/dT is nonzero only in the region close to the chemical potential. If the density of states does not vary rapidly around μ, we can use its value at $E = \mu$ and pull $D(\mu)$ out of the integration. In addition, the change of μ with temperature in metal is very small because E_f is very large. We can thus neglect the temperature dependence of μ and set $\mu \approx E_f$. Under these approximations, eq. (4.69) becomes

$$\begin{aligned} C_e &\approx D(\mu)\int_{0}^{\infty} (E - E_f)\frac{df(E, T, \mu)}{dT}dE \\ &= D(\mu)\int_{0}^{\infty} \frac{(E - E_f)(E - \mu)}{\kappa_B T^2}\frac{\exp\left(\frac{E-\mu}{\kappa_B T}\right)}{\left[\exp\left(\frac{E-\mu}{\kappa_B T}\right) + 1\right]^2}dE \\ &\approx \kappa_B^2 T D(E_f)\int_{-E_f/\kappa_B T}^{\infty} \frac{x^2 e^x}{(e^x + 1)^2}dx \end{aligned} \tag{4.70}$$

Since $E_f/\kappa_B T$ is very large, the above integral can be evaluated by setting the lower limit to $-\infty$, leading to the following expression for the specific heat

$$C_e = \frac{1}{2}\pi^2 n_e \kappa_B T/T_f \tag{4.71}$$

where $T_f = E_f/\kappa_B$ is called the *Fermi temperature*. In deriving eq. (4.71), we used the relationship $n_e = 2E_f D(E_f)/3$, which can be obtained from eqs. (3.52) and (3.53). Thus the specific heat of electrons is linearly dependent on temperature.

4.2.3 Phonons

4.2.3.1 Debye Model

In chapter 3, we obtained the phonon density of states per unit volume under the Debye approximation when the three acoustic phonon polarizations are identical [eq. (3.55)],

$$D(\omega) = \frac{dN}{V\,d\omega} = 3 \times \frac{\omega^2}{2\pi^2 v_D^3} \tag{4.72}$$

The total energy of phonons per unit volume is

$$U = \int_0^{\omega_D} \hbar\omega f\,(T,\omega) D\,(\omega)\,d\omega = \frac{3}{2\pi^2 v_D^3} \int_0^{\omega_D} \frac{\hbar\omega^3 d\omega}{\exp(\hbar\omega/\kappa_B T) - 1} \tag{4.73}$$

and the volumetric specific heat of phonons can be calculated from

$$C = \frac{\partial U}{\partial T} = \frac{3\hbar^2}{2\pi^2 v_D^3 \kappa_B T^2} \int_0^{\omega_D} \frac{\omega^4 \exp\,(\hbar\omega/\kappa_B T)}{[\exp(\hbar\omega/\kappa_B T) - 1]^2}\,d\omega \tag{4.74}$$

From eqs. (3.56) and (3.57), the Debye frequency ω_D, Debye velocity v_D, and Debye temperature θ_D are related through

$$\omega_D = \frac{\pi v_D}{a_D} = \frac{\kappa_B \theta_D}{\hbar} \tag{4.75}$$

where a_D is the effective lattice constant under the Debye model. Substituting eq. (4.75) into eq. (4.74), we get

$$C = \frac{3\hbar^2}{2\pi^2 (a_D \omega_D/\pi)^3 \kappa_B T^2} \int_0^{\omega_D} \frac{\omega^4 \exp(\hbar\omega/\kappa_B T)}{[\exp\,(\hbar\omega/\kappa_B T) - 1]^2}\,d\omega$$

$$= \frac{3\pi\kappa_B}{2a_D^3} \left(\frac{T}{\theta_D}\right)^3 \int_0^{\theta_D/T} \frac{x^4 e^x\,dx}{(e^x - 1)^2} \tag{4.76}$$

Using eq. (3.57), the specific heat can be further written as

$$C = 9\kappa_B \left(\frac{N}{V}\right)\left(\frac{T}{\theta_D}\right)^3 \int_0^{\theta_D/T} \frac{x^4 e^x dx}{(e^x - 1)^2} \tag{4.77}$$

where N/V is the number of atoms per unit volume. At low temperatures, the integration limit can be set to infinity, leading to the familiar T^3 law,

$$C(T) = \frac{36\pi^4 \kappa_B}{15}\left(\frac{N}{V}\right)\left(\frac{T}{\theta_D}\right)^3 \propto T^3 \tag{4.78}$$

Generally, the Debye temperature is unknown and the above expression is used to calculate the Debye temperature from experimentally measured values of specific heat. If the Debye model is accurate, a single value of the Debye temperature should be able to fit all of the temperature-dependent specific heat data. Such a situation happens rarely, however, and the Debye temperature is sometimes given as a function of temperature. This temperature-dependent Debye temperature is because the Debye model assumes a linear dispersion, which is not valid for phonons close to the boundary of the first Brillouin zone. In particular, it is completely wrong for optical phonons, for which the Einstein model is more appropriate, as we discuss below.

4.2.3.2 Einstein Model

Einstein's model assumes that all phonons have the same frequency ω_E and is thus more appropriate for optical phonons. We assume that there are N' states; that is, N' is the number of lattice points or primitive cells for each optical phonon polarization.* The total energy of the crystal per unit volume due to the contribution of the optical phonons with a frequency ω_E is then

$$U = N_p \frac{N' f(T, \omega_E)\hbar\omega_E}{V} = \frac{N_p N' \hbar\omega_E}{V[\exp(\hbar\omega_E/\kappa_B T) - 1]} \tag{4.79}$$

where the factor N_p accounts for the number of polarizations of optical phonons at this frequency. The specific heat per unit volume is then

$$C = \frac{\partial U}{\partial T} = N_p \kappa_B \frac{N'}{V} \frac{(\hbar\omega_E/\kappa_B T)^2 \exp(\hbar\omega_E/\kappa_B T)}{[\exp(\hbar\omega_E/\kappa_B T_B) - 1]^2} \tag{4.80}$$

The contributions of other optical phonons at a different frequency can be similarly calculated. At high temperature, both the Debye model and the Einstein model lead to the same result, as required by the equipartition theorem because the oscillator has three directions and each direction has two degrees of freedom (kinetic energy plus potential energy).

Clearly, the Debye model will be more appropriate for acoustic phonons and the Einstein model for optical phonons. At low temperatures, acoustic phonons are normally

*Notice that this N' is different from N in the Debye model, in which all phonon modes (including the optical modes) are lumped as three identical acoustic modes.

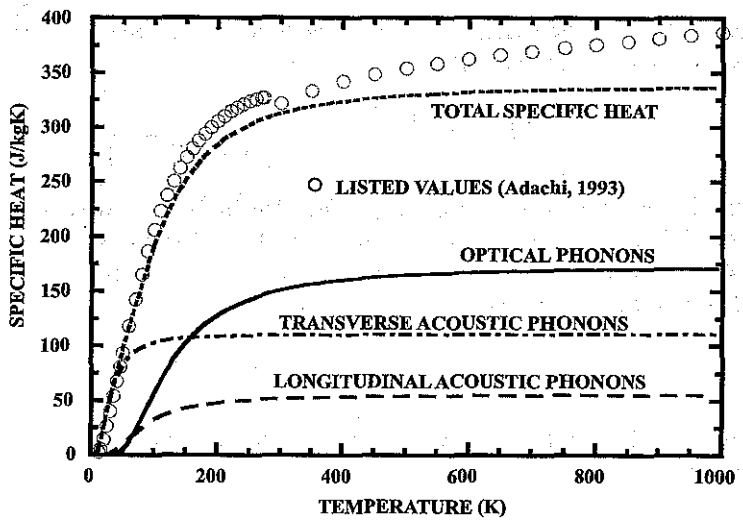

Figure 4.5 Estimated contribution of different phonon branches to the specific heat of GaAs (Chen, 1997).

excited, so the Debye approximation is more appropriate. At room and higher temperatures, both acoustic and optical phonons are excited and a combination of the two models is more appropriate. Figure 4.5 shows the estimated contributions of different phonon polarizations to the specific heat of GaAs (Chen, 1997). In this figure, a sine-function was assumed for the acoustic phonon dispersion.

4.2.4 Photons

Photons are bosons and obey the Bose–Einstein distribution. We have obtained the photon density of states in a three-dimensional cavity in eq. (3.59),

$$D(\omega) = \frac{dN}{V\,d\omega} = \frac{\omega^2}{\pi^2 c^3} \tag{4.81}$$

From eq. (4.81), the photon energy density per unit volume per unit angular frequency interval is

$$U_\omega = f(\omega, T)\hbar\omega D(\omega) = \frac{\hbar}{\pi^2 c^3}\frac{\omega^3}{[\exp(\hbar\omega/\kappa_B T) - 1]} \tag{4.82}$$

Since a photon propagates in all directions at the speed of light c, the intensity is then*

$$I_\omega = \frac{cU_\omega}{4\pi} = \frac{\hbar}{4\pi^3 c^2}\frac{\omega^3}{[\exp(\hbar\omega/\kappa_B T) - 1]} \tag{4.83}$$

*See section 6.1.3 for a more detailed explanation of intensity.

Equation (4.83) is the Planck blackbody radiation law, expressed in terms of per angular frequency interval. In terms of wavelength, we have

$$I_\lambda = I_\omega \left|\frac{d\omega}{d\lambda}\right| = \frac{C_1/\pi}{\lambda^5[\exp(C_2/\lambda T) - 1]} \tag{4.84}$$

where $C_1 = 2\pi hc^2$ and $C_2 = hc/\kappa_B$. The blackbody emissivity power that is given in eq. (1.9) can be obtained easily from the above expression for intensity through $e_\lambda = \pi I_\lambda$. Integration of eq. (4.82) for frequencies ranging from 0 to ∞ leads to the total photon energy density

$$U = \frac{4}{c}\sigma T^4 \tag{4.85}$$

where $\sigma (= 5.67 \times 10^{-8}\ \mathrm{W\,m^{-2}\,K^{-4}})$ is the Stefan–Boltzmann constant. The total intensity is

$$I = \frac{\sigma T^4}{\pi} \tag{4.86}$$

and the blackbody emissive power is thus

$$e_b = \pi I = \sigma T^4 \tag{4.87}$$

Although the concept of specific heat is seldom used in radiation, we can follow the previous treatment for electrons and phonons and calculate the photon specific heat,

$$C = \frac{16\sigma T^3}{c} \tag{4.88}$$

which has the same temperature dependence as the specific heat of phonons at low temperatures [eq. (4.78)].

Example 4.4 *Electron and phonon contributions to specific heat*

The Debye temperature of gold is 170 K and its Fermi level is 5.53 eV. Compute the specific heat of phonons and electrons in the temperature range of 0–1000 K.

Solution: The phonon and electron contributions to specific heat are given by

$$\text{Phonon: } C = 9\kappa_B \left(\frac{N}{V}\right)\left(\frac{T}{\theta_D}\right)^3 \int_0^{\theta_D/T} \frac{x^4 e^x dx}{(e^x - 1)^2}$$

$$\text{Electron: } C_e = \frac{1}{2}\pi^2 n_e \kappa_B T/T_f$$

Gold has an fcc structure with a lattice constant of 4.08 Å, and the number of atoms per unit cell is 4. Each atom contributes one valence electron. We have $n_e = N/V = 4/(4.08)^3 \times 10^{-30}\ \mathrm{m^{-3}}$. The Fermi temperature $T_f = E_f/k_B = 64$, 115 K. Substituting these numbers into the above expressions, we obtain the phonon

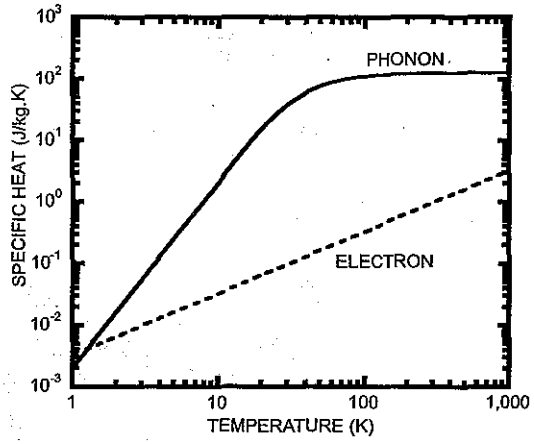

Figure E4.4 Phonon and electron contributions to the specific heat of gold.

and electron specific heats. The volumetric specific heats are converted into mass specific heat ($c = C/\rho$) and plotted in figure E4.4. We observe that the electron specific heat is typically much smaller than the phonon specific heat, except at very low temperatures.

4.3 Size Effects on Internal Energy and Specific Heat

In nanostructures, we expect that the internal energy and specific heat will be different from what we have given in the preceding sections. The differences come from two sources: one is physical and the other is mathematical. On the physics side, the energy levels, and their associated densities of states, will differ from those in bulk materials, as we have seen in chapter 3. On the mathematical side, for bulk materials we have replaced the summation over all energy states by integration in calculating the total energy. For nanostructures, this approximation may no longer be accurate.

A few experimental and theoretical studies exist about the size effects on the phonon specific heat of nanostructures. For systems of dimensionality d of 1 or higher ($d = 1$ for nanowires, $d = 2$ for films, and $d = 3$ for bulk structures), the Debye model predicts that at low temperatures the lattice specific heat should be proportional to T^d. The most common criterion for dimensional crossover is to compare the average phonon wavelength λ to the length scale of the structure. The average phonon wavelength can be estimated from the spectral-dependent phonon internal energy [the integrand of eq. (4.73)], similar to that obtaining the Wien's displacement law, eq. (1.11), from the Planck law. Well below the Debye temperature, this wavelength is given by $\lambda T \approx 50\,\text{nm K}$ for sound velocity v_s (5000 m s^{-1}). For example, a 3 nm Si thin film would be expected to exhibit $C \sim T^3$ behavior at 50 K ($\lambda \approx 1$ nm), but $C \sim T^2$ behavior at 5 K ($\lambda \approx 10$ nm). Some questions exist about whether the resulting low-dimensional specific heat should be larger or smaller than the corresponding bulk value. A simple model (Dames et al., 2004) summing over all of the normal modes of an elastic continuum with free boundaries predicts that the low-temperature specific heat of

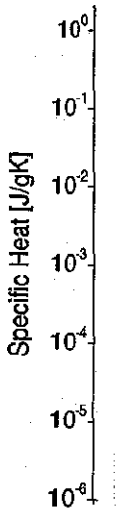

Figure 4.6 Experim
under different condi
electron micrographs

1- or 2-dimensional
predict the low-tem
to bulk (Prasher an
value (Grille et al.,
1987; Tosic et al., 1

Limited experim
on zero-dimensiona
ments (Novotny an
by 50–100% at ten
the diameter of the
asymptotic return to
fully explained by t
with free boundari
1975). For anatase
particles of about 15
experimental data o
with that of bulk Ti
temperatures (Dam

Considerable effe
(CNT). Yi et al. (19
walled (MW) CNT,
another MWCNT e
with temperatures o

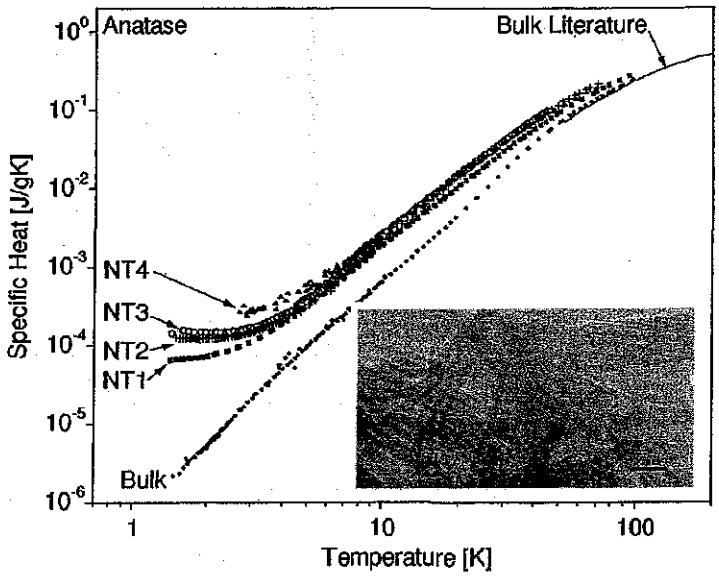

Figure 4.6 Experimental specific heat of anatase TiO_2 nanotubes (four kinds of tubes synthesized under different conditions) and that of bulk TiO_2 (Dames et al., 2004). Insert shows transmission electron micrographs of the nanotubes.

1- or 2-dimensional systems should exceed the bulk value, but several other calculations predict the low-temperature, low-dimensional specific heat should be reduced compared to bulk (Prasher and Phelan, 1998; Yang and Chen, 2000), slightly larger than the bulk value (Grille et al., 1996), or varying from both below and above bulk (Hotz and Siems, 1987; Tosic et al., 1992).

Limited experimental data are available to test these theories. The first studies were on zero-dimensional (0D) metallic nanoparticles of ~2–10 nm diameter, where experiments (Novotny and Meincke, 1973; Chen et al., 1995) show a specific heat enhanced by 50–100% at temperatures where the average phonon wavelength is comparable to the diameter of the nanoparticles, an exponential decay at lower temperatures, and an asymptotic return to bulk values at higher temperatures. These results have been successfully explained by theories that sum over all of the normal modes of an elastic sphere with free boundaries (Baltes and Hilf, 1973; Lautenschlager, 1975; Nonnenmacher, 1975). For anatase nanoparticles, Wu et al. (2001) reported enhancement by 20% for particles of about 15 nm diameter between 78 K and 370 K. In figure 4.6, we compare the experimental data on the specific heat of compacted titanium dioxide (TiO_2) nanotubes with that of bulk TiO_2, and show that the nanotubes have higher specific heat at low temperatures (Dames et al., 2004).

Considerable effort has been devoted to studying the specific heat of carbon nanotubes (CNT). Yi et al. (1999) observed a linear temperature dependence down to 10 K in multi-walled (MW) CNT, in close agreement with isolated sheets of graphene. In contrast, another MWCNT experiment by Mizel et al. (1999) showed a much steeper decay, with temperatures of about $T^{2.5}$ down to ~1 K, a better match to graphite. Bundles of

single-walled (SW) CNT were studied by both Hone et al. (2000) and Mizel et al. (1999), and exhibited a linear or slightly superlinear temperature dependence from ~100 K down to ~2–4 K. At lower temperatures, Lasjaunias et al. (2003) reported a transition to T^3 attributed to the filling up of inter-tube modes, plus a surprising additional term proportional to $T^{0.34}$ or $T^{0.62}$ below ~1 K that was qualitatively attributed to localized excitations of atomic rearrangement as in glasses and amorphous materials. In all of these CNT, the specific heat is bounded between that of graphite and graphene. Various theoretical efforts have had mixed success at explaining these MWCNT and SWCNT measurements by extending isolated tube models to include the effects of interlayer coupling (in MWCNT) and intertube coupling (Mizel et al., 1999; Hone et al., 2000; Zhang et al., 2003). Overall, more work is needed to reconcile the diverse experimental results with theory (Dresselhaus and Eklund, 2000).

In comparison with phonons, we anticipate that the specific heat of electrons will have a stronger size dependence, due to the following factors: (1) the energy quantization of electrons is more dramatic than that of phonons; (2) the specific heat also depends on the Fermi level, particularly the rate of change of the density of states at the Fermi level. In our derivation of the electron specific heat in metals, we assumed that the density of states does not change much near the Fermi level. For nanostructures, the sharp features in the electronic density of states suggest that this assumption may not be valid. Indeed, existing studies show that the specific heat is a strong function of the size (Ghatak and Biswas, 1994; Lin and Shung, 1996).

For photons, we are not interested in the specific heat but rather in the energy density or emission spectrum from small objects. Since thermal radiation can have relatively long wavelengths, the issue of size effects on the energy density of the emission spectrum from a small object has been studied for various geometries (Rytov, 1959; Rytov et al., 1989). One interesting question is whether the thermal emission from any structure at any specific wavelength can exceed the blackbody radiation given by the Planck law. For example, the density of states in photonic crystals can be very different from that in free space. It can be inferred that in the frequency region where the photon density of states of the photonic crystal is larger than that in its parent crystal, the energy density of the thermal radiation inside the photonic crystal can exceed that in its parent crystal. However, not all of the energy can be emitted into free space since the density of states in free space is limited by eq. (4.81), and thus the maximum emissive power in an open free space is the blackbody radiation. There are, however, some recent experimental reports of the far-field thermal emission from photonic crystals being larger than that of the blackbody, although the physics is not clear (Lin et al., 2003). At small scales, however, radiative heat exchange can exceed that between two blackbodies due to the tunneling of evanescent and surface waves (Polder and Van Hove, 1971; Tien and Cunnington, 1973; Pendry, 1999; Mulet et al.; 2002; Narayanaswamy and Chen, 2003), which we will discuss in more detail in the next chapter. Another example is that the emissivity of particles with a diameter comparable to the wavelength can exceed 1 because of the diffraction effect (Bohren and Huffman, 1983).

4.4 Summary of Chapter 4

Through statistical mechanics, this chapter establishes the link between the energy states and temperature for a system in equilibrium. A system in equilibrium makes

R	universal gas constant, $J\,K^{-1}\,mol^{-1}$	ω	angular frequency, rad.Hz
s	accessible quantum state	Ω	number of accessible states in a microcanonical system
S	entropy, $J\,K^{-1}$	$\mathfrak{S}$	grand canonical partition function
T	temperature, K	$\langle\rangle$	ensemble average
U	system energy, J		
v	speed, $m\,s^{-1}$		
V	system volume, m^3		
x	integration variable		
Z	canonical partition function		
θ	temperature, K		
κ_B	Boltzmann constant, $J\,K^{-1}$		
λ	thermal de Broglie wavelength, m		
μ	chemical potential, J		
ν	frequency of phonons or photons, Hz		
ρ	density, $kg\,m^{-3}$		
σ	Stefan–Boltzmann constant, $W\,m^{-2}\,K^{-4}$		

Subscripts

D	Debye
e	electronic
f	at Fermi level
i	ith energy level
r	reservoir; rotational
t	total
v	vibrational
V	constant volume
x, y, z	Cartesian coordinate direction

4.6 References

Adachi, S., ed., 1993, *Properties of Aluminum Gallium Arsenide*, INSPEC, London.

Baltes, H.P., and Hilf, E.R., 1973, "Specific Heat of Lead Grains," *Solid State Communications*, vol. 12, pp. 369–373.

Bohren, C.F., and Huffman, D.R., 1983, Absorption and Scattering of Light by Small Particles, Wiley, New York.

Callen, H.B., 1985, *Thermodynamics and an Introduction to Thermostatistics*, Wiley, New York.

Chen, Y.Y., Yao, Y.D., Hsiao, S.S., Jen, S.U., Lin, B.T., Lin, H.M., and Tung, C.Y., 1995, "Specific Heat Study of Nanocrystalline Palladium," *Physical Review B*, vol. 52, pp. 9364–9369.

Chen, G., 1997, "Size and Interface Effects on Thermal Conductivity of Superlattices and Periodic Thin-Film Structures," *Journal of Heat Transfer*, vol. 119, pp. 220–229.

Dames, C., Poudel, B., Wang, W.Z., Huang, J.Y., Ren, Z.F., Sun, Y., Oh, J.I., Opeil, C., Naughton, S.J., Naughton, M.J., and Chen, G., "Low-dimensional phonon specific heat of titanium dioxide nanotubes," submitted for publication.

Dresselhaus, M.S., and Eklund, P.C., 2000, "Phonons in Carbon Nanotubes," *Advances in Physics*, vol. 49, pp. 705–814.

Ghatak, K., and Biswas, S., 1994, "Influence of Quantum Confinement on the Heat Capacity of Graphite," *Fizika A*, vol. 3, pp. 7–24.

Grille, H., Karch, K., and Bechstedt, F., 1996, "Thermal Properties of $(GaAs)_M(Ga_{1-x}Al_xAs)_N(001)$ Superlattices," *Physica B*, vol. 119–120, pp. 690–692.

Hone, J., Batlogg, B., Benes, Z., Johnson, A.T., and Fischer, J.E., 2000, "Quantized Phonon Spectrum of Single-Wall Carbon Nanotubes," *Science*, vol. 289, pp. 1730–1733.

Hotz, R., and Siems, R., 1987, "Density of States and Specific Heat of Elastic Vibrations in Layer Structures," *Superlattices and Microstructures*, vol. 3, pp. 445–454.

Kittel, C., and Kroe[illegible]H., 1980, *Thermal Physics*, 2nd ed., Freeman, New York.

Kubo, R., Toda, M[illegible]Hashitsume, N., 1998, *Statistical Physics II*, 2nd ed., Springer, Berlin.

Lasjaunias, J.C., Biljakovic, K., Monceau, P., and Sauvajol, J.L., 2003, "Low [illegible]rgy Vibrational Excitations in Carbon Nanotubes Studied by Heat Capacity," *Nanotechnology*, vol. 14, pp. 998–1003.

Lautenschlager, R., 1975, "Improved Theory of the Vibrational Specific Heat of Lead Grains," *Solid State Communications*, vol. 16, pp. 1331–1334.

Lin, M.F., and Shung, W.W.K., 1996, "Electronic Specific Heat of Single-Walled Carbon Nanotubes," *Physical Review B*, vol. 54, pp. 2896–2900.

Lin, S.Y., Moreno, J., and Fleming, J.G., 2003, "Three-Dimensional Photonic-Crystal Emitters for Thermal Photovoltaic Power Generation," *Applied Physics Letters*, vol. 83, pp. 380–381.

Mizel, A., Benedict, L.X., Cohen, M.L., Louie, S.G., et al., 1999, "Analysis of the Low-Temperature Specific Heat of Multiwalled Carbon Nanotubes and Carbon Nanotube Ropes," *Physical Review B*, vol. 60, pp. 3264–3270.

Mulet, J.-P., Joulain, K.L., Carminati, R., and Greffet, J.-J., 2002, "Enhanced Radiative Heat Transfer at Nanometric Distances," *Microscale Thermophysical Engineering*, vol. 6, pp. 209–222.

Narayanaswamy, A., and Chen, G., 2003, "Surface Modes for Near-Field Thermophotovoltaics," *Applied Physics Letters*, vol. 82, pp. 3544–3546.

Nonnenmacher, Th.F., 1975 "Quantum Size Effect on the Specific Heat of Small Particles," *Physics Letters A*, vol. 51, pp. 213–214.

Novotny, V., and Meincke, P.P.M., 1973, "Thermodynamic Lattice and Electronic Properties of Small Particles," *Physical Review B*, vol. 8, pp. 4186–4199.

Pendry, J.B., 1999, "Radiative Exchange of Heat between Nanostructures," *Journal of Physics, Condensed Matter*, vol. 11, pp. 6621–6633.

Polder, D., and Van Hove, M., 1971, "Theory of Radiative Heat Transfer between Closely Spaced Bodies," *Physical Review B*, vol. 4, pp. 3303–3314.

Prasher, R.S., and Phelan, P.E., 1998, "Size Effects on the Thermodynamic Properties of Thin Solid Films," *Journal of Heat Transfer*, vol. 120, pp. 1078–1086.

Rytov, S.M., 1959, *Theory of Electric Fluctuations and Thermal Radiation*, Air Force Cambridge Research Center, Bedford, MA, Report AFCRC-TR-59–162.

Rytov, S.M., Kravtsov, Y.A., and Tatarskii, V.I., 1989, *Principles of Statistical Radiophysics*, vol. 3, Springer-Verlag, Berlin.

Tien, C.L., and Cunnington, G.R., 1973, "Cryogenic Insulation Heat Transfer," *Advances in Heat Transfer*, vol. 9, pp. 349–417.

Tosic, B.S., Setrajcic, J.P., Mirjanic, D.L., and Bundalo, Z.V., 1992, "Low-Temperature Properties of Thin Films," *Physica A*, vol. 184, pp. 354–366.

Wu, X.M., Wang, L., Tan, Z.C., Li, G.H., and Qu, S.S., 2001, "Preparation, Characterization, and Low-Temperature Heat Capacities of Nanocrystalline TiO_2 Ultrafine Powder," *Journal of Solid State Chemistry*, vol. 156, pp. 220–223.

Yang, B., and Chen, G., 2000, "Lattice Dynamics Study of Phonon Heat Conduction in Quantum Wells," *Physics of Low-Dimensional Structures*, vol. 5/6, pp. 37–48.

Yi, W., Lu, L., Zhang, D.-L., Pan, Z.W., and Xie, S.S., 1999, "Linear Specific Heat of Carbon Nanotubes," *Physical Review B*, vol. 59, pp. R9015–R9018.

Zhang, S., Xia, M., Zhao, S., Xu, T., and Zhang, E., 2003, "Specific Heat of Single-Walled Carbon Nanotubes," *Physical Review B*, vol. 68, 075415/1–7.

4.7 Exercises

4.1 *Grand canonical ensemble.* Establish a grand canonical ensemble and derive the probability distribution for the ensemble, that is, eq. (4.17).

4.2 *Thermal de Broglie wavelength.* Calculate the thermal de Broglie wavelength of a He molecule at 300 K and show that the dilute gas condition, eq. (4.34), is satisfied at 1 atm and 300 K.